Proceedings of the ASME 2022
International Conference on Multibody Systems, Nonlinear Dynamics, and Control
MSNDC2022
August 14–17, 2022, St. Louis, MO

IDETC2022-89185

THE FOOT IN WALKING - TOWARDS DEVELOPING A CONSTRAINED MODEL OF STANCE PHASE DYNAMICS

Daniel Renjewski[1,*], Susanne Lipfert[2], Michael Günther[3],

[1] Lecturer, Chair of Applied Mechanics, Department of Mechanical Engineering, School of Engineering and Design, Technical University of Munich, Garching, Germany
[3] Computational Biophysics and Biorobotics, Institute for Modelling and Simulation of Biomechanical Systems, University of Stuttgart, Stuttgart, Germany
[2] Section for Applied Sports Science, Department of Sports and Health Sciences, Technical University of Munich, Munich, Germany

ABSTRACT

Bipedal walking is the most prevalent form of human locomotion — versatile, robust, and efficient. However, it is a form of motion few other animals share, and plantigrade bipedalism is fairly unique to our species. Plantigrade feet play an important role in shaping the fundamental gait dynamics, and understanding their role unlocks a huge potential for biomechanical insights for locomotion research, gait rehabilitation, and humanoid robotics. Still, a comprehensive functional model of the foot, which ties the fundamental dynamics of walking to the interaction of foot and ground, does not yet exist due to the inherent mechanical complexity.
In this paper, we present a set of assumptions in detail to simplify the development of a mathematical description of the foot's motion during stance phase in human walking. These assumptions are validated using experimental data. We can show that the complex motion of the foot can be ultimately reduced to a simple rotation, which allows the formulation of a single degree of freedom equation of motion that ties proximal dynamics and constraints into a planar foot model of dynamic interactions.

Keywords: biomechanics, contact interaction, mechanical dynamics, legged robots, reduced order models, bipedal walking

NOMENCLATURE

CoM	*center of mass*
CoP	*center of pressure* - point of force application of the resulting GRF
CoR	*center of rotation* - velocity pole of the foot during stance
GRF	*ground reaction force*

*Corresponding author: Daniel.Renjewski@tum.de

1. INTRODUCTION

Early attempts to understand the fundamentals of human locomotion date back thousands of years. Apart from various motivations, we assume a common scientific curiosity at the core of biomechanics to understand an impressive mechanism that has evolved without any immediately conceivable design strategy or input, let alone a clearly defined design objective.
The foot has been studied concerning various aspects of its role in bipedal human walking, e.g., [1–3], and key functions have been identified:

- ➔ support and stability [4–6],
- ➔ increasing stride length and energy conversion [2, 7, 8],
- ➔ reducing the contact collision [9], and
- ➔ absorbing the impact by forceful plantarflexion [10, 11].

The functions listed above have been devised from experimental observations, and derived from design constraints imposed by control requirements of bipedal machines [12].
These analytic approaches revealed certain aspects of the foot mechanics, but especially modern bipedal robots often attach a foot rather for anthropomorphic than for functional reasons and fail to reproduce the intricate dynamics of natural human gait. Mathematical models of bipedal gait, on the other hand, might suggest that a foot is entirely unnecessary to reproduce human walking dynamics [13], while omitting fundamental features like the shifting CoP.
We hypothesize that, by synthesizing a functional mechanical model of the foot, a deeper understanding of its function as part of the dynamic interaction of body and ground can be achieved. Towards that end, we aim at reducing the complexity of the whole interacting system as much as possible, while still capturing its fundamental dynamical properties [14].

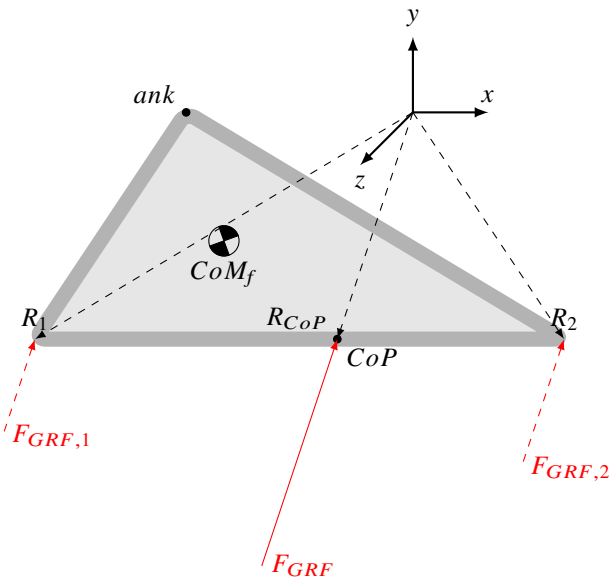

FIGURE 1: A SCHEMATIC REPRESENTATION OF THE PLANAR FOOT MODEL WITH THE GRF ACTING AT THE COP, ITS DISTRIBUTION SHOWN BY TWO DASHED FORCE VECTORS AT BOTH ENDS OF THE FOOT WITH THEIR RESPECTIVE POSITION VECTORS SHOWN IN BLACK.

This encompasses the proposal of a foot model with as few degrees of freedom as possible, in order to clear the way for a most compact formulation of the foot's equation of motion.

2. FUNDAMENTALS OF FOOT MODELING: GRF, COP, AND COR

The foot is a multi-segmented, articulated body with all sorts of connective tissue and non-primitive joints [4]. On the one hand, its evolutionary history [2], along with its intrinsic complexity and versatile application in various gaits, hampers the identification of fundamental functions for a specific gait. On the other hand, simplifications like curved feet [15] or the complete omission of feet [16] in robots indicate a functional underappreciation of the role of the foot in walking.

2.1 Fundamentals

GRF distribution in a contact plane. The foot in stance applies forces to the ground and is, for all intends and purposes, the major link that allows changes in momentum of the locomoting human. The interaction between foot and ground is most accurately described as a force distribution but can be simplified to a resulting ground reaction force (GRF) with the center of pressure (CoP) as the point of force application. An inherent part of this compacted formulation of the foot-ground interaction is that only one additional factor, the yaw torque about the CoP, is required to fully capture the contact mechanics. In its simplest form, the position of the CoP can be modeled, without loss of generality, by assuming two separate forces applied at two distinct points of the foot, fixed in space. Accordingly, we consider the GRF vector $\vec{F}_{GRF}$ to consist of exactly two distinct contributions:

$$\vec{F}_{GRF} = \vec{F}_{GRF,1} + \vec{F}_{GRF,2} \quad . \tag{1}$$

These contributions are assumed to act at spatially separated points of application $\vec{R}_1$ and $\vec{R}_2$, respectively, in a transversal plane, most commonly assumed at ground level. To reduce the complexity of modeling, we restrict full generality by introducing the additional parameter β and, assuming parallelism, define

$$\vec{F}_{GRF,1} = |\beta| \cdot \vec{F}_{GRF,2} \tag{2}$$

for both $\vec{F}_{GRF}$-contributions, which yields

$$\vec{F}_{GRF} = (1 + |\beta|) \cdot \vec{F}_{GRF,1} \quad . \tag{3}$$

Equation (3) implies [17, 18], [19, eqs. 2]

$$\begin{aligned} \vec{R}_{CoP} &= \frac{F_{GRF,1,n}}{F_{GRF,1,n} + F_{GRF,2,n}} \cdot \frac{\beta}{|\beta|} \cdot \vec{R}_1 \\ &\quad + \frac{F_{GRF,2,n}}{F_{GRF,1,n} + F_{GRF,2,n}} \cdot \vec{R}_2 \\ &= \frac{\beta}{1 + |\beta|} \cdot \vec{R}_1 + \frac{1}{1 + |\beta|} \cdot \vec{R}_2 \end{aligned} \tag{4}$$

where $F_{GRF,i,n}$ are the components normal to the ground of each contributing force share. As mentioned above, the two points of force application $\vec{R}_1$ and $\vec{R}_2$ are treated as fixed anatomical-geometrical parameters, with their distance specifying a characteristic length of the body contacting the ground, i.e., the foot.
The position $\vec{R}_{CoP}$ of the net CoP is always defined for a flat plane of contact between two bodies. Equation (4) formulates the sum of all single force application positions $\vec{R}_i$ of all force contributions $\vec{F}_{GRF,i}$, with each $\vec{R}_i$ (here: $\vec{R}_1$ and $\vec{R}_2$) being weighted by the respective force component $F_{GRF,i,n}$ normal to the plane. In case $\beta = 0$, the model would simplify to having incorporated just one GRF contribution $\vec{F}_{GRF} = \vec{F}_{GRF,2}$, which acts exactly at $\vec{R}_{CoP} = \vec{R}_2$.

Velocity pole A velocity pole, also referred to as the *instant center of rotation* (COR), is a point in space around which all points of a body pivot. In other words, given it's current velocity, the body's movement can be described as a pure rotation around this point in this particular instant. A translational motion is equivalent to a rotation with infinite radius, and its velocity pole is located at the end of parallel pole beams. Composed motions, as e.g., rolling, exhibit well-defined but time-dependent instantaneous CoRs. Accordingly, time-invariant CoRs can be found for bodies executing a pure rotation around an axis fixed in space. This kind of rotation is characterized by time-invariant distances between the CoR and points of the rotating body i

$$|\vec{R}_{CoR,i}| = const. \tag{5}$$

In order to simplify the model of the foot's motion during stance phase in walking, we hypothesize that a time-invariant velocity pole exists. This hypothesis is explicitly assumed to be not valid for early stance from the instant the heel strikes the ground until the entire foot is firmly planted and flat on the ground.
For the purpose of identifying this velocity pole, we apply a nonlinear least-square fit to experimental data. As points of the foot for which we require constant distances around the velocity

pole (Eq. 5), we select the experimentally measured ankle joint position $\vec{R}_{Ank}$ and the derived CoM position of the foot $\vec{R}_{CoM,f}$ [20] (see. Fig. 1).
The deviation $d(t)$ from the assumed constant vector length can be expressed as

$$\begin{aligned} d_{CoM,f}(t) &= R_{CoM,f} \\ &\quad -\sqrt{(x_{CoM,f}-x_c)^2+(y_{CoM,f}-y_c)^2} \\ d_{Ank}(t) &= R_{Ank}-\sqrt{(x_{Ank}-x_c)^2+(y_{Ank}-y_c)^2}, \end{aligned} \quad (6)$$

where $R_{CoM,f}$ and R_{Ank} are the time-invariant Euclidian distances between the CoR and the experimentally determined foot's center of mass (CoM) and the ankle, respectively; the vectors $(x_{CoM,f}, y_{CoM,f})^T$ and $(x_{Ank}, y_{Ank})^T$ are the time-dependent positions of the respective landmarks, and $(x_c, y_c)^T$ is the position of the time-invariant velocity pole.
An optimization problem based on Eq. (6) for determining R_{Ank}, $R_{CoM,f}$, x_c, and y_c was formulated as

$$\underset{R_{Ank},R_{CoMf},x_c,y_c}{\operatorname{argmin}} \sum_t \left| d_{Ank}(t) \cdot d_{CoMf}(t) \right| \quad (7)$$

and solved for these four parameters using *lsqnonlin* in Matlab2020b (The Mathworks, Nattick (MA), USA) for each captured experimental walking step individually. The formulation of the objective in terms of a product of deviations (Eq. (7)) turned out to yield particularly consistent optimization results.

Functional considerations for the GRF components. Generally, $\vec{R}_{1,2}$ can be treated as free parameters in the CoP modeling considerations presented above. Yet, with the ultimate aim of simplifying the equations of motion of the foot, we introduce the point $\vec{R}_{con}$ as a fixed CoR (a geometric constraint), to be identical with $\vec{R}_2$. The distributed force components thus receive specific functional meaning, with the geometric constraint to be maintained by exactly the force $\vec{F}_{GRF,con}$, which therefore inherits the character of a constraint force. The vector $\vec{F}_{GRF,1}$, on the other hand, marks an active force, from here on denoted as $vecF_{GRF,act}$, with R_{act} as the respective point of application, to be identical with $\vec{R}_1$.
For further simplification, we assume that the origin of the coordinate system be located at the CoR, i.e., $\vec{R}_{con}=0$, which makes Eq. (4) contract to

$$\vec{R}_{CoP} = \frac{\beta}{1+|\beta|} \cdot \vec{R}_{act} \quad . \quad (8)$$

Thus, implying $\vec{R}_{con}=0$, the number of model parameters that specify the $\vec{F}_{GRF}$ distribution at the ground can be reduced to just β and $\vec{R}_{act}=(R_{act,x},0)=(-\ell_f,0)$, with the length $\ell_f > 0$ being a natural suggestion for fixing the absolute value of $\vec{R}_{act}$ (solely its horizontal component in our case).
The distribution of forces can then be calculated from Eq. (3) as

$$\vec{F}_{GRF,act} = \frac{\vec{F}_{GRF}}{1+|\beta|} \quad (9)$$

and (Eq. (2))

$$\vec{F}_{GRF,con} = \vec{F}_{GRF} - \vec{F}_{GRF,act} \quad (10)$$

.

3. METHODS

In Sec. 2.1, we have established the basis to simplify the mathematical description of the foot during stance phase in human walking by identifying a velocity pole and constraining the motion to one degree of freedom. In order to verify this assumption we have used experimental data of human subjects walking at normal speed.

3.1 Experimental protocol

Experimental data had been recorded in a previous study [21], in which three-dimensional (3D) lower limb kinematics and GRFs were collected from 21 subjects (11 females, 10 males) walking on an instrumented treadmill (type ADAL-WR, HEF Tecmachine, Andrezieux Boutheon, France) at 75% of their preferred transition speed between walking and running (approximately $1.5\,\mathrm{m\,s^{-1}}$, which corresponds to a good approximation of normal walking speed). The study had been approved by the University of Jena Ethics Committee (in accordance with the Declaration of Helsinki), and written informed consent was provided by all subjects prior to the experiments. Subjects wore athletic footwear in which they felt comfortable, and they were given ample time for warming up and getting familiar with the treadmill. None of the participants reported any case of locomotor deficit.

Motion analysis was performed using eight wall-mounted high-speed infrared cameras (Qualisys, Gothenburg, Sweden) recording at a sampling frequency of 240 Hz. For the present study, we used the recorded sagittal positions of four reflective markers placed over anatomical landmarks on each of the subject's lower limbs, respectively.

Marker kinematics and GRF data were recorded simultaneously, with both measuring systems' data sets being synchronized by a trigger signal provided by the treadmill computer. The remaining time delay (2.5×10^{-3} s) and time drift ($2.0\times10^{-5}\,\mathrm{s\,s^{-1}}$) between both systems were identified and corrected after the measurements [22].

3.2 Velocity pole determination

Based on landmark data and after having performed initial marker processing [23, appendix], the optimization problem according to Eq. 7 was solved. In order to calculate meaningful data in accordance with the scope of our hypothesis, an appropriate time period for fitting had to be determined for each step. Accordingly, the period during which the foot rotates in terminal stance, while still maintaining contact with the ground, had to be identified beforehand. The onset of rotation was determined as the moment in time when the foot starts to move, after a period of being firmly planted on the ground. As an indicator, we used the vertical velocity of the ankle marker pointing up (beyond noise: ϵ) for the first time in stance

$$t_{start} = t\left(\frac{dy_{Ank}}{dt} > \epsilon\right). \quad (11)$$

For determining the derivative, the numerical gradient of the data using the sample frequency f_s was calculated. The end of stance phase was determined from GRF-data at the instant when the vertical force dropped below 0 N. To account for inaccuracies in

force measurement during very late stance phase, the final three samples were omitted

$$t_{stop} = t(GRF_y < 0) - 3 \cdot \frac{1}{fs}. \quad (12)$$

In order to execute the optimization, by means of Eq. 7, $x_{CoM,f}(t)$, $y_{CoM,f}(t)$, $x_{Ank}(t)$, $y_{Ank}(t)$ were taken from experimental measurements throughout the time period determined beforehand $t = [t_{start}, t_{stop}]$, and initial values $[x_{c,0}, y_{c,0}, R_{CoM,f,0}, R_{Ank,0}]$ of the searched parameters were chosen as

- $x_{c,0}$ ➔ the most anterior position of the fifth metatarsal joint marker during stance phase,
- $y_{c,0}$ ➔ the experimental ground height,
- $R_{COM,f,0}$ ➔ 0.2 m, and
- $R_{Ank,0}$ ➔ 0.3 m,

respectively. The optimization search space for each parameter was bound to the intervals of (±0.3 m,±0.3 m,[0.05,0.4]m,[0.1,0.5]m). The bounds were set as to not restrict the optimizer while still keeping a sufficiently small and meaningful search space. This has been confirmed by checking that no optimization results appeared near or at the search space boundaries.

The optimization was executed using *lsqnonlin* in MATLAB2020b (trust-region-reflective algorithm, max. iterations: 2000, function tolerance 10^{-9}, max. evaluations: 10^6, optimality tolerance [24]: 10^{-9}).

The quality of the result was, on the one hand, determined from the squared norm of the residual, normalized to the number of considered samples (Δt)

$$R_{res,opt} = \frac{\Delta t}{t_{stop} - t_{start}} \cdot \sum_t (d_{Ank}(t) \cdot d_{CoM,f}(t))^2, \quad (13)$$

and on the other hand as the deviations $d_{Ank}(t)$ and $d_{CoM,f}(t)$, each normalized to its optimized distance (lever length) R_{Ank} and $R_{CoM,f}$, respectively, for each sample

$$err = \frac{d_i}{R_i}, i = CoM, f; Ank \quad (14)$$

.

3.3 Force distribution and CoP

In order to calculate the force distribution, we fixed the application point $\vec{R}_{act} = (-\ell_f, 0)$ of the action force without loss of generality at an arbitrary length estimate $\ell_f > 0$ of the foot: 1.2-times the distance from the CoR to the heel of the projected foot determined by the initial position $R_{CoP,p}$ of the CoP. We then determined $\beta(t)$ from Eq. 8:

$$\beta(t) = \begin{cases} \dfrac{-R_{CoP,x}}{1.2 \cdot \ell_f + R_{CoP,x}} & R_{CoP,x} < 0 \\ \dfrac{-R_{CoP,x}}{1.2 \cdot \ell_f - R_{CoP,x}} & R_{CoP,x} \geq 0 \end{cases}. \quad (15)$$

The force distribution between $F_{GRF,act}$ and $F_{GRF,con}$ was then calculated from Eqs. 9 and 10.

	single subjects		all subject		
event	avg.	std.	avg.	std.	unit
steps	57	-	1143	-	[1]
t_{step}	0.93	0.02	0.98	0.05	s
TO_c	12.06	0.85	11.44	1.00	% GC
TD_c	50.55	0.75	50.45	1.12	% GC
TO	62.01	0.82	61.19	1.00	% GC

TABLE 1: STEP TIMING COMPARISON FOR A SINGLE SUBJECT AND ALL SUBJECTS. THE NUMBER OF STEPS AND THEIR AVERAGE DURATION ARE SHOWN AS WELL AS THE INSTANCE OF THE FOLLOWING GAIT EVENTS: TAKE-OFF OF THE CONTRALATERAL LEG (TO_c), TOUCH-DOWN OF THE CONTRALATERAL LEG (TD_c), AND TAKE-OFF OF THE IPSILATERAL LEG (TO)

.

4. RESULTS

This paper exposes key methodical steps that carve out essentials of human walking dynamics by reflecting them in the mechanical variables of a reductionist foot model. This model is derived from foot properties and behavior as observed in experiments. The validity of the proposed methods is demonstrated in the following experimental analysis. For readability, all figures depict results for a single, representative (see Table 1) subject.

4.1 Velocity pole

For each step, the number of samples that has been taken into account in each optimization, depending on the instant of foot rotation onset (see Sec. 2.1), averages to (25.9 ± 4.7) samples with a minimum of 7 and a maximum of 46 samples considered (Fig. 2). The resulting residual is documented (Fig. 3) individually for the optimization period as well as the entire period from the onset of single support phase to the end of the optimization period. The average residual (Eq. 13) amounts to $(0.3505 \pm 0.3422) \times 10^{-10}\text{m}^4$, i.e., a mean of 1.8 mm deviation from the optimized foot lever lengths ($R_{CoM,f}$ and R_{Ank}) at each sample. The location of velocity poles for all steps of a single subject along with the normalized deviation (Eq. 14) for all samples is shown in Fig. 3.

For each step, a time-invariant velocity pole can be found on average (10.1 ± 1.2) cm in front and (6.6 ± 0.7) cm below the most forward position of the Mt5 marker during flat-foot phase (see Fig.3). The step-specific CoRs of all subjects scatter within a radius of 2 cm around the median. The resulting vector lengths measured from the respective CoRs were (20.50 ± 0.14) cm to the foot's CoM ($|\vec{R}_{CoM,f}|$) and (26.80 ± 0.44) cm to the ankle joint ($\vec{R}_{Ank}$). The mean percentage residuals for all considered samples were (0.42 ± 0.34) % of the optimized foot lever length during the optimization phase, and (1.24 ± 1.07) % during the single support plus optimization phases.

4.2 CoP projection

The CoR defines a new virtual ground level, which allows to consistently model the interaction between foot and environment via a CoP defined on a flat surface. For the purpose of determining a CoP in this plane, this point of action of the GRF is transferred, maintaining its torque applied on the foot, from the CoP, determined experimentally in the plane of the force platform, along the GRF's line of action into the x-z-plane that contains the

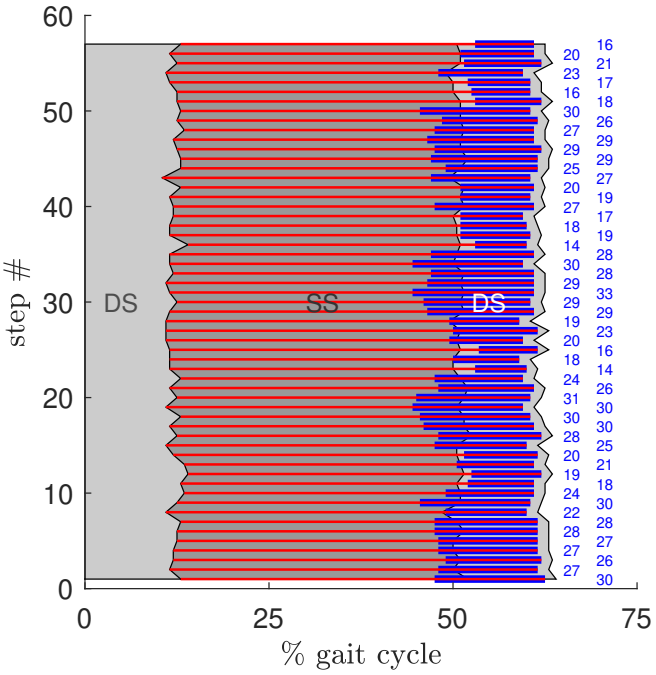

FIGURE 2: STEP TIMING FOR ALL (57) RECORDED STEPS OF A SINGLE SUBJECT. THE SINGLE SUPPORT PHASE (SS) IS PRECEDED AND FOLLOWED BY DOUBLE SUPPORT PHASES (DS), INDICATED BY THE GRAY SHADED AREAS, IN EARLY AND LATE STANCE. BLUE BARS INDICATE THE PERIOD FOR WHICH EXPERIMENTAL DATA OF THIS STEP HAVE BEEN USED TO DETERMINE THE OPTIMIZED CoR POSITION IN THIS SPECIFIC STEP; THE NUMBER OF SAMPLES ARE NOTED RIGHT TO THE RESPECTIVE BAR. THE RED BAR INDICATES THE PERIOD FOR WHICH THE RESIDUAL OF MEASURED VERSUS OPTIMISED LEVER LENGTH HAS BEEN CALCULATED.

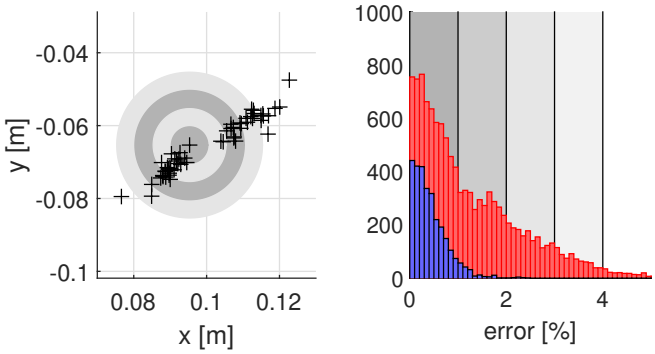

FIGURE 3: DISTRIBUTION OF OPTIMIZED CoRs FOR 57 STEPS OF A SINGLE SUBJECT (LEFT PANEL). CIRCLES INDICATE DEVIATIONS IN STEPS OF 0.5 CM AROUND THE MEDIAN CoR. EACH CROSS INDICATES THE OPTIMIZED CoR FOR A STEP. IN THE RIGHT PANEL, THE RESIDUAL PER SAMPLE IN % RELATIVE TO THE OPTIMIZED LEVER LENGTH OF BOTH LEVER ARMS IS SHOWN FOR EACH SAMPLE DURING THE OPTIMIZATION PERIOD (2862 SAMPLES, IN BLUE), AS WELL AS DURING THE ENTIRE SINGLE SUPPORT PLUS OPTIMIZATION PERIOD (11 560 SAMPLES, IN RED).

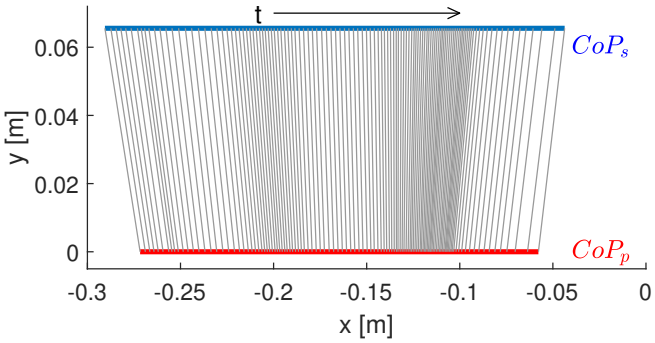

FIGURE 4: TRANSFER OF THE EXPERIMENTALLY MEASURED CoP AT THE GROUND (EXPRESSED IN TERMS OF COMPONENTS W.R.T. THE CoR-COORDINATE SYSTEM CoP*s*) INTO THE PLANE THROUGH THE CoR PARALLEL TO THE GROUND (CoP*p*) FOR ALL SAMPLES DURING STANCE.

CoR (Fig. 4). Since we choose the CoR as the origin for a shifted inertial reference frame and accordingly shift the experimentally determined position vectors, the CoP transfer can be performed by first solving

$$\begin{bmatrix} F_{GRF,x} & -1 & 0 \\ F_{GRF,y} & 0 & 0 \\ 0 & 0 & -1 \end{bmatrix} \cdot \begin{pmatrix} u \\ v \\ w \end{pmatrix} = \begin{pmatrix} R_{CoP,x,s} \\ R_{CoP,y,s} \\ 0 \end{pmatrix} \qquad (16)$$

for u. In this linear system of equations, $F_{GRF,x/y}$ denotes the GRF components in the saggital plane, and $R_{CoP,x/y,s}$ the experimentally determined CoP position expressed in terms of components w.r.t. the inertial reference frame that originates at the CoR. The CoP transferred into the latter reference frame (CoP_p) (shift along $\vec{F}_{GRF}$: preservation of the torque on the foot by $\vec{F}_{GRF}$) is then calculated as

$$\begin{pmatrix} R_{CoP,x,p} \\ R_{CoP,y,p} \\ 0 \end{pmatrix} = \begin{pmatrix} R_{CoP,x,s} \\ R_{CoP,y,s} \\ 0 \end{pmatrix} + u \cdot \begin{pmatrix} F_{GRF,x} \\ F_{GRF,y} \\ 0 \end{pmatrix}. \qquad (17)$$

4.3 Force distribution and CoP

In accordance with the forward (anterior) shift of the CoP progressing during stance phase, β decreases over the time of stance phase. Correspondigly, the force distribution shifts from being applied more posteriorly to an equal distribution just before midstance, with the force acting at the constraining CoR (at $\vec{R}_{con}$) ultimately prevailing (Fig. 5). The CoP does not reach the CoR as the CoR is located well anteriorly to the metatarsal joint, but the decreasing GRF in late stance reduces the absolute difference between $F_{GRF,con} = |\vec{F}_{GRF,con}|$ and $F_{GRF,act} = |\vec{F}_{GRF,act}|$.

5. DISCUSSIONS

The reduction of the mechanical description of the foot's motion during stance in human walking addresses a major issue in understanding the foot's function. Current models of the foot are either too simple and cannot capture its dynamic contribution, or they are overly complex, thus obscuring the key functionality. By reducing the foots motion to a single degree of freedom and transforming the experimentally measured dynamics into a plane parallel to the ground, which contains the velocity pole, a reduced order equation of motion can now be formulated using Newton's

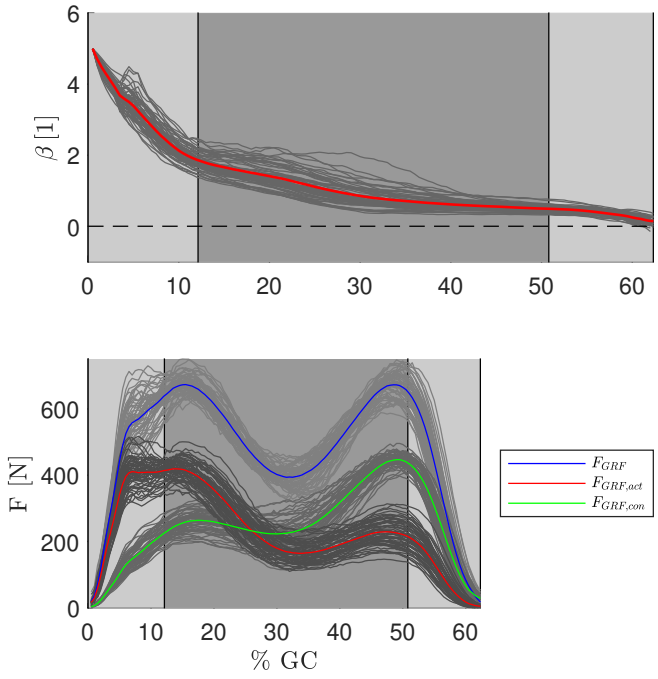

FIGURE 5: FORCE DISTRIBUTION COEFFICIENT (β) DURING STANCE PHASE AND FORCE DISTRIBUTION AT BOTH POINTS OF APPLICATION($\vec{R}_{act}$ AND $\vec{R}_{con}$).

law's of motion — a dynamic and reductionist foot model. At the same time, the force distribution within the GRF gives additional functional insights and can reveal characteristic properties that will be helpful to develop controllers for humanoid robots, enabling them to generate more for human-like, versatile motion. Beyond the work detailed in this paper, our approach offers mechanical considerations that allow the formulation of mechanical equations that describe the foot's fundamental dynamics during stance at various degrees of complexity, with the aim of gaining insights into the intricate interplay of active forces that result from proximal segment dynamics and constraints imposed by the ground.

Such insights will ultimately enhance our understanding of the foot's key role in the versatile and robust walking gait that is quite unique to humans. This will benefit the improvement of gait rehabilitation as well as the development of gait-assistive devices and walking robots.

6. CONCLUSIONS

In this paper, we have shown how the dynamics of the foot in single and final double support during human walking lend themselves to be described as a pure rotation around a velocity pole. This pole is, within reasonable bounds, time-invariant throughout a single step, but varies slightly in-between different steps. The naturally occurring restriction of the foot's generally superposing linear and angular motions to only a rotation (the occurrence of a pole) facilitates the exact determination of the distribution between an active (posterior) and constraint (anterior) contribution to the GRF. The introduced force distribution parameter (β) depends on only two landmarks, namely the assumed point of force application of the active force (somewhere at the heel) and the experimentally determined position of the pole (CoR).

ACKNOWLEDGMENTS

Funding: This work was supported by the German Research Foundation (DFG) under grants 449427815, and 234087184. **Author contributions:** SL conducted all experiments, SL, MG and DR analyzed the biomechanics data, DR and MG developed the analytical model and prepared the manuscript. All authors revised and approved the final manuscript. **Competing interests:** All authors declare to have no competing interests. **Data and materials availability:** The data supporting the main conclusions of the manuscript are included in the manuscript and supplementary material.

REFERENCES

[1] Hohmann, Georg. *Fuß und Bein*. Springer (1951).

[2] Holowka, Nicholas B. and Lieberman, Daniel E. "Rethinking the evolution of the human foot: insights from experimental research." *The Journal of Experimental Biology* Vol. 221 No. 17. DOI 10.1242/jeb.174425.

[3] Zelik, K. E. and Honert, E. C. "Ankle and foot power in gait analysis: Implications for science, technology and clinical assessment." *J Biomech* Vol. 75 (2018): pp. 1–12. DOI 10.1016/j.jbiomech.2018.04.017. URL https://www.ncbi.nlm.nih.gov/pubmed/29724536.

[4] Bähler, André. "The biomechanics of the foot." *Clinical Prosthetics and Orthotics* Vol. 10 No. 1 (1984): pp. 8–14.

[5] McKeon, P. O., Hertel, J., Bramble, D. and Davis, I. "The foot core system: a new paradigm for understanding intrinsic foot muscle function." *British Journal of Sports Medicine* Vol. 49 No. 5 (2015): pp. 290–298. DOI 10.1136/bjsports-2013-092690. URL https://www.ncbi.nlm.nih.gov/pubmed/24659509.

[6] Davis, S. and Caldwell, D. G. "The Design of an Anthropomorphic Dexterous Humanoid Foot." *IEEE/RSJ 2010 International Conference on Intelligent Robots and Systems (IROS 2010)* (2010): pp. 2200–2205DOI Doi 10.1109/Iros.2010.5649756. URL <GotoISI>://WOS:000287672000051.

[7] Bullimore, S.R. and Burn, J.F. "Consequences of forward translation of the point of force application for the mechanics of running." *Journal of Theoretical Biology* Vol. 238 No. 1 (2006): pp. 211–219.

[8] Ker, R. F., Bennett, M. B., Bibby, S. R., Kester, R. C. and Alexander, R. M. "The spring in the arch of the human foot." *Nature* Vol. 325 No. 7000 (1987): pp. 147–149. DOI 10.1038/325147a0. URL https://www.ncbi.nlm.nih.gov/pubmed/3808070.

[9] Salathé, Eric P., Arangio, George A. and Salathé, Eric P. "The foot as a shock absorber." *Journal of Biomechanics* Vol. 23 No. 7 (1990): pp. 655–659. DOI 10.1016/0021-9290(90)90165-y.

[10] Messenger, Neil. "Moving the human machine: understanding the mechanical characteristics of normal human walking." *Physics Education* Vol. 29 No. 6 (1994): pp. 352–357.

[11] Donelan, J.M., Kram, R. and Kuo, A.D. "Mechanical and metabolic determinants of the preferred step width in human walking." *Proceedings of the Royal Society of London B* Vol. 268 No. 1480 (2001): pp. 1985–1992.

[12] Vukobratović, Miomir and Borovac, Branislav. "Zero-Moment Point — Thirty Five Years of Its Life." *International Journal of Humanoid Robotics* Vol. 01 No. 01 (2012): pp. 157–173. DOI 10.1142/s0219843604000083.

[13] Geyer, H., Seyfarth, A. and Blickhan, R. "Compliant leg behaviour explains basic dynamics of walking and running." *Proceedings of the Royal Society of London B* Vol. 273 No. 1603 (2006): pp. 2861–2867.

[14] Full, R. J. and Koditschek, D. E. "Templates and anchors: neuromechanical hypotheses of legged locomotion on land." *J Exp Biol* Vol. 202 No. Pt 23 (1999): pp. 3325–32. DOI 10.1242/jeb.202.23.3325. URL https://www.ncbi.nlm.nih.gov/pubmed/10562515.

[15] Martin, Anne E., Post, David C. and Schmiedeler, James P. "Design and experimental implementation of a hybrid zero dynamics-based controller for planar bipeds with curved feet." *The International Journal of Robotics Research* Vol. 33 No. 7 (2014): pp. 988–1005. DOI 10.1177/0278364914522141. URL https://dx.doi.org/10.1177/0278364914522141.

[16] Hubicki, Christian, Grimes, Jesse, Jones, Mikhail, Renjewski, Daniel, Spröwitz, Alexander, Abate, Andy and Hurst, Jonathan. "ATRIAS: Design and validation of a tether-free 3D-capable spring-mass bipedal robot." *The International Journal of Robotics Research* Vol. 35 No. 12 (2016): pp. 1497–1521. DOI 10.1177/0278364916648388.

[17] Cavanagh, P R. "A technique for averaging center of pressure paths from a force platform." *Journal of Biomechanics* Vol. 11 No. 10-12 (1978): pp. 487–491.

[18] Winter, D A. *Biomechanics and Motor Control of Human Movement*, 4. ed. John Wiley & Sons, New York (2009).

[19] Günther, M, Otto, D, Müller, O and Blickhan, R. "Transverse pelvic rotation during quiet human stance." *Gait & Posture* Vol. 27 No. 3 (2008): pp. 361–367. DOI 10.1016/j.gaitpost.2007.05.014.

[20] Hahn, Ulrich. "Entwicklung mehrgliedriger Modelle zur realistischen Simulation dynamischer Prozesse in biologischen Systemen." Diplomathesis, Eberhard-Karls-Universität, Tübingen. 1993. Available online [1].

[21] Lipfert, Susanne W. *Kinematic and Dynamic Similarities between Walking and Running*. Verlag Dr. Kovač Hamburg (2010).

[22] Lipfert, S W, Günther, M and Seyfarth, A. "Diverging times in movement analysis." *Journal of Biomechanics* Vol. 42 No. 6 (2009): pp. 786–788. DOI 10.1016/j.jbiomech.2008.12.020.

[23] Lipfert, S W, Günther, M, Renjewski, D and Seyfarth, A. "Impulsive ankle push-off powers leg swing in human walking." *The Journal of Experimental Biology* Vol. 217 No. Pt 8 (2014): pp. 1218–1228. DOI 10.1242/jeb.097345. Correction: 10.1242/jeb.107391.

[24] Nocedal, Jorge and Wright, Stephen. *Numerical optimization*. Springer Science & Business Media (2006).

[1] https://biomechanicsbiorobotics.info/tatbiomechanik/publ/dipl/ulihahn/diplom_uli_hahn.pdf